Biophysical Chemistry, 33 (1989) 195–204
Elsevier

BPC 01354

Ca^{2+}-dependent regulation of the dynamic polarity of F-actin under the influence of tropomyosin and troponin

Koshin Mihashi, Naoya Suzuki and Atsushi Ooi

Laboratory of Molecular Biophysics, Department of Physics, Faculty of Science, Nagoya University, Chikusa-ku, Nagoya 464-01, Japan

Received 1 November 1988
Revised manuscript received 20 January 1989
Accepted 23 January 1989

Actin regulation, F-; Subunit exchange; Pyrenyl-actin; Dynamic polarity; Ca^{2+}-dependent regulation

A novel method that we have developed in the preceding paper to study the subunit exchange rates of F-actin (N. Suzuki and K. Mihashi, Biophys. Chem. 33 (1989) 177) was applied to regulated F-actin (a complex of F-actin, tropomyosin and troponin). We found that the dynamic polarity of regulated F-actin is modulated in a Ca^{2+}-dependent manner, giving rise to strong suppression of the on/off rates of subunit exchange at the P-end. We interpreted this characteristic suppression as follows. Removal of Ca^{2+} from troponin C in regulated F-actin produces strong constraints on fluctuations in potential energy of an intermediate conformation of the terminal structure (P-end) which would be formed in the course of association and dissociation of the actin subunit.

1. Introduction

The free energy for skeletal muscle contraction is supplied by ATP hydrolysis on cross-bridges, or myosin heads, which protrude from thick filaments. The key intermediate in this reaction, myosin-ADP-P_i, is believed to form an energized complex with F-actin in thin filaments. The energy liberated is transformed into the macroscopic work done in sliding of two filaments under load. During the course of formation of the energized complex, activation of the local motion of F-actin occurs. The directional motion of the individual actin subunit of F-actin would be essential for sliding of the cross-bridge to occur along F-actin [1].

A number of previous studies on both the complex of F-actin, tropomyosin and troponin (the so-called regulated F-actin) in vitro and thin filament in vivo have revealed that the flexural rigidity of F-actin increases markedly when Ca^{2+} is removed from troponin C on the filament [2–4]. Earlier spectroscopic investigations of F-actin using a triplet probe have demonstrated the torsional flexibility of F-actin [5,6], indicating that F-actin is more flexible when undergoing twisting motion than bending motion. This anisotropic flexibility of F-actin becomes Ca^{2+}-dependent under the influence of the regulatory proteins, tropomyosin and troponin [5,7]. Since the flexibility of F-actin (both flexural and torsional) is based on the fluctuation of coupling between actin subunits, the observed modulation of flexibility by a tropomyosin and troponin ($\pm Ca^{2+}$) system suggests that coupling between actin subunits in regulated F-actin is susceptible to the concentration of free Ca^{2+} associated with the Ca^{2+} receptivity of troponin C. At the terminals of F-actin, fluctuations in the coupling actin subunits gives rise to a probability of terminal actin subunits exchanging with G-actin in the solution. Therefore, we expect that subunit exchange at the terminal of regulated F-actin is also Ca^{2+}-dependent. The first evidence

Correspondence address: K. Mihashi, Laboratory of Molecular Biophysics, Department of Physics, Faculty of Science, Nagoya University, Chikusa-ku, Nagoya 464-01, Japan.
Abbreviation: PIAA, *N*-(1-pyrenyl)iodoacetamide.

in support of this mechanism in vitro was obtained in a previous study [8] in which the use of a sensitive fluorescence assay led to the observation that the rate of incorporation of G-actin into regulated F-actin under near-steady-state conditions is significantly reduced when the concentration of free Ca^{2+} is reduced below $pCa = 7$. This change was immediately reversed upon addition of sufficient Ca^{2+}. These results indicate that although troponin C is not located at the terminal of F-actin, the Ca^{2+} receptivity of troponin C is transmitted very rapidly to the terminal actin subunits. The details of this mechanism are investigated in the present study by the application of a new fluorescence method that we have developed for quantitative analysis of the on/off rate constants of subunit exchange at the terminals of F-actin under quasi-steady-state conditions [9]. By exploiting the high sensitivity of the fluorescent probe, we were able to determine the extent of label incorporation into F-actin to a detectable threshold as low as a few subunits/filament. Our results show that the changes in on/off rate constants at the P-end are associated with the Ca^{2+}-receptivity of troponin C, while the on/off rate constants at the B-end are not affected significantly. This phenomenon is sensitive to environmental conditions, indicating that the Ca^{2+}-dependent directional constraint is exerted on actin subunits in the direction of the P-end by regulatory proteins. On the basis of the present results, we would like to propose a model in which subunit exchange (both on- and off-events) at the P-end is accelerated by structural fluctuations of F-actin.

2. Methods

2.1. Theory for incorporation of labeled G-actin into F-actin under quasi-steady-state conditions

Details of the principle involved have been reported in the preceding paper [9], and therefore in the present article we shall restrict ourselves to a brief summary of the procedure.

Let us consider the case where we add a small amount of fluorescence-labeled G-actin (C_0) to a solution of F-actin which is under steady-state conditions for subunit exchange. The fluorescence intensity of the probe increases on incorporation of the actin subunit into F-actin. If preferential incorporation between labeled and unlabeled subunits does not occur and the fluorescence change is equal at both ends, the rates of incorporation of label at both ends (V_B and V_P) are expressed analogously to eq. 10 of ref. 9 by:

$$V_B(t) = A(t)\left[k_B^+ C(t) - k_B^-\right] \quad (1)$$

$$V_P(t) = A(t)\left[k_P^+ C(t) - k_P^-\right] \quad (2)$$

where $A(t)$ denotes the fraction of labeled G-actin in the total G-actin at time t. The V terms are given with respect to the rate of the label incorporation at both ends of single F-actin. As incorporation of label proceeds, the total G-actin concentration (labeled plus unlabeled) decreases, thereby approaching C_s (critical concentration). Consequently, the rate of label incorporation decreases gradually. However, during very early stages in incorporation (50–120 s after addition of label), where the amount of G-actin incorporated is only a few percent of the initial, total G-actin concentration, we are able to determine the initial rate of label incorporation (fluorescence increase) according to:

$$\frac{1}{A(0)} \left.\frac{d FI_{B+P}(t)}{dt}\right|_{t\to 0} = m\left[(k_B^+ + k_P^+)(C_s + C_0) - (k_B^- + k_P^-)\right] \quad (3)$$

$$\frac{1}{A(0)} \left.\frac{d FI_P(t)}{dt}\right|_{t\to 0} = m\left[k_P^+ (C_s + C_0) - k_P^-\right] \quad (4)$$

where m is the proportionality constant for the relation between incorporation of label and increase in fluorescence. Eqs. 3 and 4 indicate that the initial fluorescence increase divided by $A(0)$ is linearly dependent on the initial G-actin concentration ($C_s + C_0$).

As shown below, the critical concentrations of the B- and P-ends of regulated F-actin are very similar, i.e., $C_B = C_s = C_P$. In this case (case A in ref. 9), if both ends of F-actin are free to exchange subunits, then the rate of label incorporation is given by [9]:

$$V = V_B + V_P \quad (5)$$

In the presence of cytochalasin D, which caps the B-end and thus suppresses subunit exchange at the site, the rate of label incorporation is described by the following expression:

$$V = V_P \quad (6)$$

Therefore, by addition of an appropriate initial G-actin concentration relative to C_s (or C_P), we can evaluate V_B and V_P as a function of $(C_s + C_0)$. Subsequently, by using eqs. 1–4, we obtain the rate constants k_B^+, k_B^-, k_P^+ and k_P^-.

2.2. Materials and methods

The procedure for the preparation of actin from rabbit skeletal muscle and the labeling of the Cys-374 residue with *N*-(1-pyrenyl)iodoacetamide followed that described in the preceding paper [9]. A fraction of native tropomyosin (a complex of tropomyosin and troponin) was prepared according to the method of Ebashi and Ebashi [10].

In order to prepare a complex of regulated F-actin, G-actin was mixed with native tropomyosin at an actin/native tropomyosin molar ratio of 5 : 1) in low salt solution containing 200 μM ATP, 100 μM $CaCl_2$, 2 mM $NaHCO_3$ and 2 mM 2-mercaptoethanol and then dialyzed against a large volume of high salt solution containing 100 μM ATP, 60 mM KCl, 2 mM $MgCl_2$, 15 mM Tris-acetate (pH 7.6) and 2 mM 2-mercaptoethanol overnight in a cold room (5 °C). The stock solution of regulated F-actin thus prepared was used after dialysis vs. each specified solution.

ATPase activity was assayed similarly to that described in the preceding paper [9].

Adjustment of p*Ca*: to 2 ml of regulated F-actin solution at 33 °C, 20 μl of either $CaCl_2$ (10 mM) or EGTA (100 mM) was added. These solutions are henceforth referred to as 'high-Ca' or 'low-Ca' solution, respectively. The solutions were incubated for 5 min at 33 °C immediately before fluorescence measurement.

3. Results

3.1. Steady-state G-actin concentration of regulated F-actin

Regulated F-actin, in which 5% of the actin subunits are labeled with PIAA, was multiply diluted to give lower actin concentrations by using buffer M, containing 0.5 mM $MgCl_2$, 50 μM $CaCl_2$, 200 μM ATP, 5 mM Tris-HCl (pH 8.0), 1 mM 2-mercaptoethanol and 1 mM NaN_3. Under these salt conditions, we were able to add various

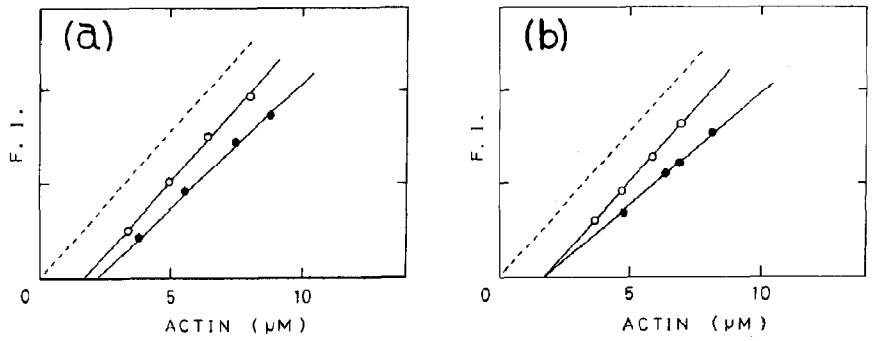

Fig. 1. Steady-state G-actin concentration of regulated F-actin solution at 33 °C. (a) High-Ca solution, containing 150 μM $CaCl_2$ and buffer M (0.5 mM $MgCl_2$, 1 mM NaN_3, 1 mM 2-mercaptoethanol, 200 μM ATP, 5 mM Tris-HCl; pH 8.0). The regulated F-actin solution in high salt solution containing 60 mM KCl and 1 mM $MgCl_2$ (in which 5% of the actin subunits were pyrene-labeled actin) was multiply diluted with buffer M and incubated in a cold room (5 °C) for 2 days. Prior to fluorescence measurements, the solution was incubated at 33 °C for 8 h. Adjustment of p*Ca* was made 5 min before fluorescence measurement. (- - - - -) Fluorescence intensity 5 min after addition of $MgCl_2$ (5 mM); this was performed in order not to include denatured actin in the steady-state concentration of G-actin. (○) In the absence of cytochalasin D. (●) Cytochalasin D (final concentration 1 μM) was added prior to incubation in the cold room. F.I., fluorescence intensity. (b) Low-Ca solution, containing 1 mM EGTA and buffer M. Other conditions as in panel a.

amounts of labeled G-actin, since the steady-state concentration of G-actin was relatively high (1–2 μM, see fig. 1). The solutions of regulated F-actin were incubated for 2 days in a cold room (5° C) and for 8 h at 33° C in order to attain steady-state conditions prior to recording fluorescence.

In high-Ca solution, the steady-state G-actin concentration of regulated F-actin amounted to 1.7 ± 0.1 μM (fig. 1a). In this determination, full polymerization of regulated F-actin was examined by addition of $MgCl_2$ (5 mM) to each solution in order to ascertain the extent of denaturation of F-actin during the prolonged incubation at 33° C. The proportion of denatured F-actin, which amounted to less than 5% of the initial concentration of F-actin, was subtracted from the total actin concentration (fig. 1a). The steady-state concentration of G-actin in high-Ca solution, determined in the presence of 1 μM cytochalasin D, was 2.1 ± 0.1 μM which is slightly greater than that in its absence (fig. 1a).

In low-Ca solution, the steady-state G-actin concentration (1.7 μM) was equal to that in high-Ca solution (fig. 1a and b). The presence of 1 μM cytochalasin D had no effect on the steady-state concentration of G-actin, however, the fluorescence intensity demonstrated a decrease of about 20% (fig. 1b). The reason for this is not clear. Further addition of cytochalasin D did not change C_s in low-Ca solution, indicating that the disparity in critical concentrations of the B- and P-ends substantially disappeared in low-Ca solution (table 1).

We reported in the preceding paper [9] that the disparity in critical concentrations of B- and P-ends is markedly reduced by binding of tropomyosin to F-actin. Additionally, we observed in the present study that when the concentration of KCl was increased, the disparity in critical concentrations of the opposite ends was virtually abolished on binding of tropomyosin plus troponin even in high-Ca solution (60 mM KCl, 1 mM $MgCl_2$, 50 μM $CaCl_2$, 200 μM ATP, 10 mM Tris-HCl (pH 8.0), 1 mM NaN_3 and 1 mM 2-mercaptoethanol at 33° C) (fig. 2).

During prolonged incubation (8 h) in buffer M at 33° C, ATP hydrolysis resulted in a maximum concentration of approx. 40 μM (conditions; 12 μM regulated F-actin in high-Ca solution). However, addition of excess ATP (500 μM) to each solution did not change the steady-state G-actin concentration.

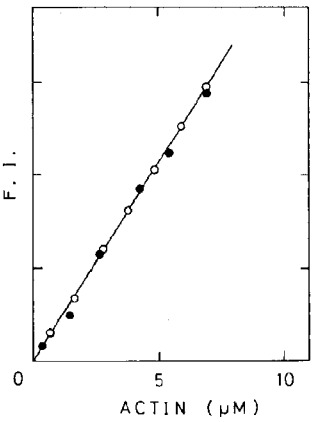

Fig. 2. Steady-state concentration of G-actin in a solution of regulated F-actin at high salt concentration. 60 mM KCl, 1 mM $MgCl_2$, 50 μM $CaCl_2$, 200 μM ATP, 10 mM Tris-HCl (pH 8.0), 1 mM NaN_3 and 1 mM 2-mercaptoethanol at 33° C. (○) In the absence of cytochalasin D; (●) in the presence of 1 μM cytochalasin D. F.I., denotes fluorescence intensity.

3.2. *Limitation of amount of labeled G-actin added*

In determinations of the rate of label incorporation, it is important to limit the amount of G-actin added in order to avoid spontaneous polymerization. We observed that, in buffer M at 33° C, G-actin at concentrations up to 4.9 μM did not undergo spontaneous polymerization, even though the fluorescence assay is sensitive enough to polymerization to detect a threshold of as little as a few subunits/filament (fig. 3). Hence, in the following experiments, 50–200 μl of a solution of labeled G-actin (protein concentration 30–50 μM) was mixed gently but rapidly with 3 ml regulated F-actin solution.

3.3. *Determination of rate of label incorporation into regulated F-actin in both high- and low-Ca solutions*

The stock solution of regulated F-actin was diluted with buffer M such that the concentration of F-actin was equal to 12 μM, and then in-

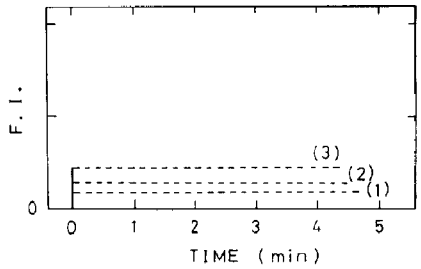

Fig. 3. Spontaneous polymerization of G-actin in buffer M at 33° C. Various amounts of G-actin (in which 5% of pyrenyl-G-actin was included) were added in buffer M at $t = 0$, and the fluorescence intensity (F.I.) was monitored continuously. G-actin added at: (1) 1.2, (2) 2.5 and (3) 4.9 μM. We note that no spontaneous polymerization was detectable until at least 4 min after mixing of G-actin, even at 4.9 μM G-actin.

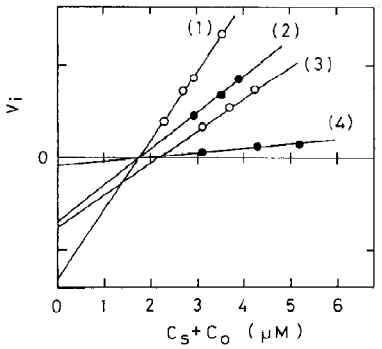

Fig. 4. Initial rate of incorporation of label divided by $A(0)$; V_i was plotted as a function of the initial concentration of total G-actin ($C_s + C_0$). Initial rate of label incorporation was determined over the time range 1–2 min after addition of labeled G-actin. In this range, a steady-state increase of fluorescence was observed which was related to total G-actin in eqs. 3 and 4. (1) High-Ca; (2) low-Ca; (3) high-Ca; 1 μM cytochalasin D; (4) low-Ca, 1 μM cytochalasin D. Ordinate given as the average rate of label incorporation of single F-actin. In calculations, the regulated F-actin concentration equal to 2 nM was used according to ref. 9 and the results of Suzuki and Mihashi (in preparation).

cubated as described above for attaining steady state. To 3 ml regulated F-actin in high-Ca solution, labeled G-actin at various final concentrations was added (viz., 0.63, 1.0, 1.24 and 1.82 μM). The initial rate of label incorporation for each solution was analysed according to eqs. 3 and 4 as a function of initial G-actin concentration ($C_s + C_0$). The resulting plots were linear, intersecting at a G-actin concentration of 1.7 ± 0.1 μM (fig. 4, line 1). This result is in line with that predicted using eqs. 3 and 4. In the presence of 1 μM cytochalasin, the initial rate of label incorporation resulted in a straight line which intersects at a point corresponding to the critical concentration of the P-end, 2.1 ± 0.1 μM (fig. 4, line 3). Increasing levels of cytochalasin D (up to 5 μM) gave essentially identical results, indicating that the effect of capping of the B-end of regulated F-actin was saturated at a cytochalasin D concentration of less than 1 μM.

In low-Ca solution, the rate of label incorporation into regulated F-actin was slower as compared to high-Ca solution over the range of G-actin concentrations studied (fig. 4, line 2). This is quite compatible with previous data demonstrating that the change in concentration of Ca^{2+} in the solution induced an instantaneous change in rate of label incorporation into regulated F-actin [8]. The presence of cytochalasin D (1 μM) in low-Ca solution resulted in a very slow rate of label incorporation (fig. 4, line 4).

The data obtained in both high- and low-Ca solutions were subjected to analysis according to eqs. 5 and 6, with the results for the B- and P-ends being depicted separately in figs. 5 and 6. The rate constants obtained are summarised in table 1. We note that Ca^{2+}-dependent regulation is very extensive at the P-end, whereas the effect at the B-end

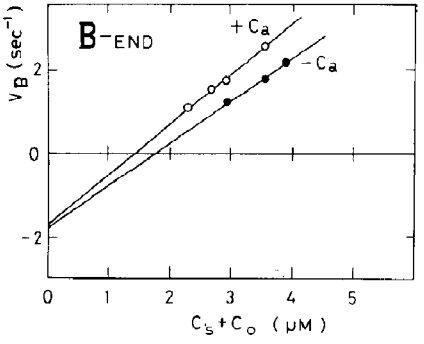

Fig. 5. Ca^{2+}-dependent change in rate of subunit incorporation at the B-end (V_B) of regulated F-actin under high-Ca (+Ca) and low-Ca (−Ca) conditions. Data point for (+Ca) were obtained by applying eqs. 5 and 6 for the experimental results of lines 1 and 3 in fig. 4. Similarly, data for (−Ca) were derived from the results of lines 2 and 4 in fig. 4.

Table 1

Kinetic parameters of subunit exchange of regulated F-actin under steady-state conditions

C_s, steady-state concentration of G-actin. C_B[rate], C_P[rate] and C_s[rate] denote the values calculated from k_B^+, k_B^-, k_P^+ and k_P^- obtained experimentally.

Parameters	Conditions			
	0.5 mM $MgCl_2$ (high-Ca), 5 mM Tris-HCl (pH 8.0)	0.5 mM $MgCl_2$ (low-Ca), 5 mM Tris-HCl (pH 8.0)	2 mM $MgCl_2$ (high-Ca), 10 mM KCl, 5 mM Tris-HCl (pH 8.0)	2 mM $MgCl_2$ (high-Ca), 30 mM KCl, 15 mM Tris-acetate (pH 7.6)
k_B^+ (M^{-1} s^{-1})	1.2×10^6	1.1×10^6	2.3×10^6	1.1×10^6
$k_B^+C_s$ (s^{-1})	2.1	1.8	1.6	0.28
k_B^- (s^{-1})	1.7	1.8	1.5	0.25
C_B[rate] (μM)	1.5	1.7	0.64	0.25
k_P^+ (M^{-1} s^{-1})	1.2×10^6	0.15×10^6	0.83×10^6	0.28×10^6
$k_P^+C_s$ (s^{-1})	1.9	0.26	0.56	0.14
k_P^- (s^{-1})	2.3	0.26	0.63	0.40
C_P[rate] (μM)	2.0	1.7	0.75	0.38
C_P (μM)	2.1	1.7	0.8	–
C_s[rate] (μM)	1.8	1.7	0.67	0.25
C_s (μM)	1.7	1.7	0.65	–
Flow (s^{-1})	0.4	0	0.2	0.3

is unremarkable, at least under the present conditions. The instantaneous change in label incorporation of regulated F-actin on addition (or removal) of Ca^{2+} observed in the previous work [8] is now readily understood as being the result of a drastic Ca^{2+}-dependent change in the values of k_P^+ and k_P^-.

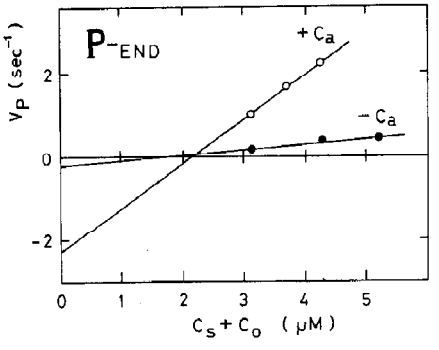

Fig. 6. Ca^{2+}-dependent change in rate of subunit incorporation at the P-end (V_P) of regulated F-actin under high-Ca (+Ca) and low-Ca (−Ca) conditions. Data points for (+Ca) and (−Ca) are depicted simply from the results for lines 3 and 4 in fig. 4.

3.4. Temperature dependence of rate constants

We observe in table 1 that the rate constant for incorporation at the B-end is apparently lower than that of the diffusion-limited process of formation of a collisional complex. This phenomenon is of greater significance at the P-end. This suggests that the rate of formation of new terminal structure is limited by a process of slow isomerization which follows the formation of a collisional complex between G-actin and the terminal actin subunits. In other words, an activation process (or processes) for the collisional complex is involved in the overall reaction of subunit incorporation at the terminals.

In fact, Arrhenius plots of the association rate constants for both B- and P-ends led to values of the activation energy that were apparently greater than the thermal energy kT (fig. 7). The magnitude of the activation energy varies widely depending on solvent conditions (see legend to fig. 7). These results indicate that an intermediate

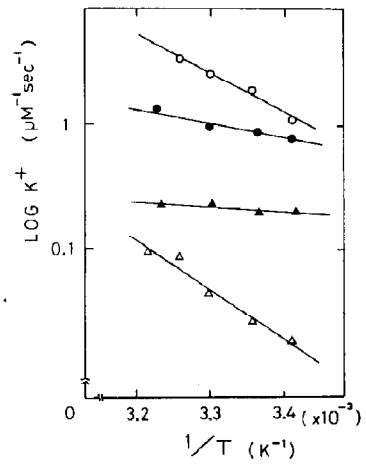

Fig. 7. Temperature dependence of k_B^+ (○, ●) and k_P^+ (△, ▲) of regulated F-actin in 'Mg' solution. (○, △) 0.5 mM $MgCl_2$, 100 μM $CaCl_2$, 200 μM ATP, 15 mM Tris-HCl (pH 8.0), 1 mM NaN_3. Activation energies calculated from the slopes of the plots were 15.3 kcal/mol for k_B^+ (○) and 19.0 kcal/mol for k_P^+ (△). In 'K/Mg' solution (●, ▲) 30 mM KCl, 2 mM $MgCl_2$, 100 μM $CaCl_2$, 200 μM ATP, 15 mM Tris-acetate (pH 7.6). Activation energies calculated from the slopes were 6.1 kcal/mol for k_B^+ (●) and 1.4 kcal/mol for k_P^+ (▲). To 2 ml of 7 μM regulated F-actin solution under steady-state conditions, 0.3 ml labeled G-actin (31 μM) solution was added and the initial rate of label incorporation was determined. The same measurement was carried out in the presence of 1 μM cytochalasin D. Knowing the steady-state concentration of G-actin (which was insensitive to temperature at least under the present solvent conditions), the observed rate of label incorporation k_{app} was converted to k^+ at both B- and P-ends using

$$k_{app} = k^+(C_s + C_0) - k^-$$

where C_0 is the amount of G-actin added (labeled and unlabeled).

state(s) of the terminal structure is created during the course of association of actin subunits with the terminal. Probably, a similar intermediate state(s) is formed during dissociation of the terminal actin subunit.

3.5. ATPase activity of regulated F-actin associated under steady-state conditions

The above results demonstrate that subunit exchange at the terminal of regulated F-actin is strongly dependent on the Ca^{2+} receptivity of troponin C. It would be interesting to establish whether the process of Ca^{2+}-dependent subunit exchange is tightly coupled to ATP hydrolysis. ATPase activity of regulated F-actin solution was assayed at 33°C in both high- and low-Ca solutions which contained 2 mM $MgCl_2$, 10 mM KCl, 50 μM $CaCl_2$ (or 1 mM EGTA), 200 μM ATP, 5 mM Tris-HCl (pH 8.0), 1 mM NaN_3 and 1 mM 2-mercaptoethanol. These data demonstrate that the average rate of ATP hydrolysis for single regulated F-actin amounts to 0.04 s^{-1} in high-Ca solution, assuming that ATPase occurs on regulated F-actin. This value is more than 40-fold smaller than the rate of the subunit 'in-flow' reaction at the B-end ($k_B^+ C_s = 1.6$ s^{-1}, table 1), indicating that the association reaction is not closely coupled to ATP hydrolysis. The rate of ATPase is still lower than the net subunit in-flow ($\simeq 0.2$ s^{-1}). These data therefore suggest that not only does incorporation of G-actin occur mostly in the form of G-actin-ATP but also release of actin subunit takes place in the form of this complex, at least under the experimental conditions employed. The result obtained in low-Ca solution is striking, since no appreciable ATPase activity occurs in spite of the occurrence of subunit exchange reaction. In this case, the net subunit flow from the B- to P-end is essentially zero; i.e., for regulated F-actin where troponin is devoid of Ca^{2+}, the subunit exchange reaction proceeds as a simple diffusion process at the terminals.

4. Discussion

4.1. Directional constraints in subunit-subunit coupling exerted on actin subunits by regulatory proteins

In this study, we have confirmed our previous data showing the rate of subunit incorporation at the terminal of regulated F-actin to be under the control of Ca^{2+}-dependent regulation by tropomyosin and troponin [8]. Additionally, in the present study we discovered that Ca^{2+}-dependent regulation is of greater significance for the P-end (cf. figs. 5 and 6). The Ca^{2+}-receptive state of troponin C switches on the 'gate' for subunit exchange at the P-end; the signal of Ca^{2+} reception on troponin C which arrives at the P-end

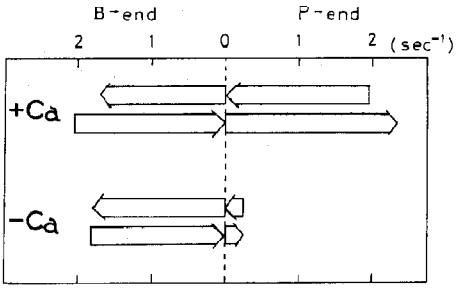

Fig. 8. The subunit-flow diagram for regulated F-actin under steady-state conditions. From the on/off rate constants of regulated F-actin (table 1), steady-state subunit inflow and outflow at both ends were calculated according to the following relations: (B-end) $k_B^+ C_s$ (inflow), k_B^- (outflow). (P-end) $k_P^+ C_s$ (inflow), k_P^- (outflow). We note that Ca^{2+}-dependent regulation is at the P-end, while it is less effective at the B-end.

switches on the gate. The signal transferred to the P-end evokes the activation of structural fluctuations. In other words, structural fluctuations elicited by troponin C upon Ca^{2+} binding are propagated along regulated F-actin. As a consequence, the subunit flow appears in the direction from the B- to P-end (fig. 8).

4.2. *Structural fluctuation at the P-end of F-actin*

The subunit-flow diagram for regulated F-actin (fig. 8) clearly demonstrates that Ca^{2+}-dependent regulation is far more important at the P-end as compared to the B-end. We note that when a Ca^{2+}-receptive signal from troponin C arrives at the P-end, both k_P^+ and k_P^- increase in approximately equal proportions (8–9-fold; table 1).

In order to elucidate the possible mechanism underlying this regulation, we shall discuss two models in the following text. The first one involves two distinct conformational states present at the P-end of F-actin depending on the Ca^{2+}-receptive state of troponin C:

$$\text{Reg-FA}(+\text{Ca}) \underset{k_f}{\overset{k_r}{\rightleftarrows}} \text{Reg-FA}(-\text{Ca})$$

here, both conformations are in dynamic equilibrium and the rate constants k_f and k_r depend on the concentration of free Ca^{2+}. We may assume that the on-rate constant for subunit exchange differs between both conformations. A similar assumption is made concerning the off-rate constant. As an extreme case, we assume that association of actin subunits occurs primarily with Reg-FA(+Ca) whereas dissociation of subunits takes place from Reg-FA(−Ca). This is described in fig. 9 (model A).

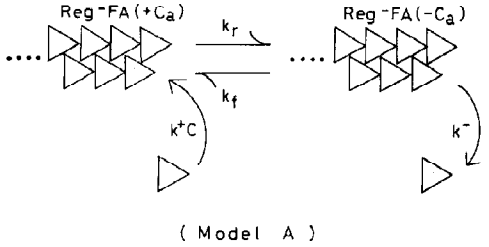

Fig. 9. Schematic diagram of the extreme case in model A.

We assume that both states, Reg-FA(+Ca) and Reg-FA(−Ca), exist in a rapid equilibrium (k_r, $k_f \gg k^+C$, k^-). Hence, the fraction of Reg-FA(+Ca) is given by $k_f/(k_r + k_f)$ with that of Reg-FA(−Ca) being expressed as $k_r/(k_r + k_f)$. The average rate of subunit incorporation is then given by

$$V = k^+ C \frac{k_f}{k_r + k_f} - k^- \frac{k_r}{k_r + k_f} \qquad (7)$$

This equation predicts that when the concentration of free Ca^{2+} decreases, the fraction in the Reg-FA(+Ca) state diminishes and consequently the apparent on rate (the first term) falls, whereas the apparent off rate (the second term) increases. The experimental results obtained in the present study, however, demonstrate that both on and off rate constants change in a parallel manner (table 1). Thus, model A does not explain the experimental results.

The second model takes into consideration a possible intermediate state (or states) suggested by the temperature dependence of the association rate constants (fig. 7). We assume that the terminal subunit must be activated to reach a transient conformational state in which the structural potential energy is much greater than those of both stable F-actin subunit and G-actin in solution. The reaction may be described as follows:

$$\text{G} + \text{P} \rightleftarrows (\text{G} - \text{P}) \rightleftarrows (\text{G}' - \text{P}') \rightleftarrows \text{P} - \text{P}$$

(model B)

where G denotes G-actin in solution, and P the terminal subunit at the P-end of F-actin. When association of G-actin occurs (reaction proceeding from left to right), the newly bound subunit (G) and the preexisting terminal subunit (P) form a collisional complex (G – P) which then undergoes activation to an intermediate complex (G′ – P′). The potential energy of the complex (G′ – P′) is higher than that of the stable configuration of the terminal (P – P). Thus, the reaction from (G′ – P′) to (P – P) is a downhill process. On the other hand, there is a chance of the terminal subunit (P) being activated to state G′ and of activation of the next subunit to state P′ from state P (reaction from right to left). Actin subunits in the G′-state may dissociate into the solution or return to state P at the terminal. The overall reaction rates for association and dissociation depend on the differences in potential according to (fig. 10):

$$k^+ \propto \exp[-(U_M - U_D)/kT]$$
$$k^- \propto \exp[-(U_M - U_A)/kT] \quad (8)$$

where U_D, U_M and U_A represent the potential of actin subunit in the dissociated, transiently activated and polymeric state, respectively. One of the essential assumptions made in this model is that both U_M and U_A do not remain constant but undergo variation due to structural fluctuations (or flexibility) in F-actin. For a description of this situation, we introduce the following potentials:

$$U_D = 0$$
$$U_M = U_{M,0} + (1/2)aE(t) \quad (9)$$
$$U_A = U_{A,0} + aE(t)$$

Here, for simplicity, we take $U_D = 0$ and the fluctuational potential energy $E(t)$ is divided into U_M and U_A (fig. 10). a denotes the coupling constant. Substitution of this potential into the rate equation leads to:

$$k^+ = k_0^+ \exp\{-bE(t)\}$$
$$k^- = k_0^- \exp bE(t) \quad (10)$$

where $b = a/(2kT)$. The experimentally observed rate constant is the average of the fluctuating values of k;

$$\langle k^+ \rangle = k_0^+ \langle \exp\{-bE(t)\} \rangle \quad (11)$$
$$\langle k^- \rangle = k_0^- \langle \exp bE(t) \rangle \quad (12)$$

If $E(t)$ shows a Gaussian distribution profile, we have

$$\langle \exp bE(t) \rangle = \langle \exp\{-bE(t)\} \rangle$$
$$= \exp\{(1/2)b^2 \langle E^2(t) \rangle\} \quad (13)$$

which is a positive value. This means that both the on and off reactions will be accelerated simultaneously by structural fluctuations of F-actin. The acceleration increases in extent with larger structural fluctuations. This is precisely the behavior observed in the current study. The Ca^{2+}-dependent increases in on/off rate constants at the P-end occur in parallel, in line with expectation (table 1). Thus, model B is very reasonable.

We are able to describe the quantitative aspects of amplification of the directional fluctuations of F-actin. Eqs. 11–13 can be rewritten as follows:

$$(\langle k^+ \rangle / k_0^+) = \exp(b^2 \langle E^2(t) \rangle / 2) \quad (14)$$

Here we make use of the analogy between the Ca^{2+}-dependent activation with the thermal activation of fluctuation (eq. 14), thereby deriving the relation:

$$(k_P^+(+Ca))/(k_P^+(-Ca))$$
$$= (k_P^-(+Ca))/(k_P^-(-Ca))$$
$$= \exp(a^2 \langle E^2(t) \rangle / 8(kT)^2) \quad (15)$$

The ratio for the rate constants between the high- and low-Ca solutions amounts to 7.8 for k_P^+ and 9.4 for k_P^- (table 1). In eq. 15, E represents the

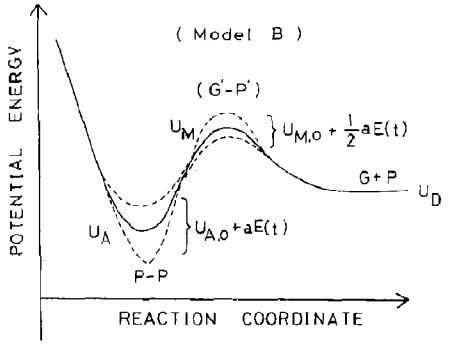

Fig. 10. Schematic diagram of the structural potential profile of the P-end to explain the observed association and dissociation of actin subunits (model B).

difference in potential energy fluctuations observed between high- and low-Ca solutions. If we choose the coupling constant a as being equal to unity, the ratio of rate constants calculated above gives $E = 4.2kT$ at the P-end, with the result for the B-end being negligible. In conclusion, the activation energy for both on and off reactions and the fluctuations in potential at the P-end are significantly greater than those at the B-end (table 1). This description therefore details the basic characteristics of the dynamic polarity of regulated F-actin.

4.3. Biological implications of Ca^{2+}-dependent regulation of the dynamic structure of the P-end

(i) In the contractile mechanism for skeletal muscle: in the contractile system of actomyosin, a myosin cross-bridge slides along F-actin in the direction from the P- to B-end [11]. Interestingly, the direction coincides with that of the directional fluctuations of actin subunits revealed in the present study. Both sliding of the myosin head and directional fluctuations of actin subunits are regulated by the tropomyosin/troponin/($\pm Ca^{2+}$) system. It may be suggested that the local motion of actin subunits (translational and/or rotational) which underlies the change in k_P^+ and k_P^- is of great importance for the translational motion (sliding) of the myosin head along F-actin. It is possible that the elementary motion of the myosin head during sliding may consist not only of translation along F-actin, but also of limited rotation around the actin subunit.

It should be noted that in the case of skeletal muscle, the P-end of the thin filaments is bound to β-actinin [12]. We have no knowledge of the type of modulation brought about in the contraction of muscle when β-actinin is removed from the tip of thin filaments. In our model analysis presented above (model B), the energy fluctuation elicited by the troponin system amounts to $4.2kT$. If the end-capping β-actinin acts as a 'clip' at the P-end of F-actin, an enormous amount of elastic energy will be stored in thin filaments which can be regulated by the action of troponin.

(ii) The newly suggested function of the 'B-end capping proteins': it has already been discussed that the B-end capping proteins stabilize F-actin by suppressing subunit exchange at the B-end where subunit exchange occurs at a high frequency (relative to the low-frequency site of the P-end). In the preceding paper [9], we showed that stabilization of F-actin may be afforded by tropomyosin which 'does not cap' the B-end but binds laterally to F-actin. Interestingly, suppression by tropomyosin was observed on the P-end instead of the B-end. Moreover, on inclusion of troponin, Ca^{2+}-dependent regulation was demonstrated at the P-end as is shown in the present study. It appears that the P-end is more sensitive to environmental changes than is the B-end (table 1 and fig. 8 in ref. 9). From these considerations, we postulate that the function of the B-end capping proteins is to render F-actin susceptible to subtle changes in environment through the P-end by means of capping the high-frequency site of the B-end (bias toward high-frequency noise; a kind of low-pass filter). This type of function for the B-end capping proteins has not been previously proposed.

Acknowledgement

We are most indebted to Professor F. Oosawa for stimulating discussions during the preparation of this paper.

References

1 F. Oosawa, S. Fujime, S. Ishiwata and K. Mihashi, Cold Spring Harbor Symp. Quant. Biol. 37 (1973) 277.
2 S. Ishiwata and S. Fujime, J. Mol. Biol. 68 (1972) 511.
3 S. Yoshino, Y. Umazume, R. Natori, S. Fujime and S. Chiba, Biophys. Chem. 8 (1978) 317.
4 T. Yanagida and F. Oosawa, J. Mol. Biol. 126 (1978) 507.
5 K. Mihashi, H. Yoshimura, T. Nishio, A. Ikegami and K. Kinosita, Jr, J. Biochem. 93 (1983) 1705.
6 H. Yoshimura, T. Nishio, K. Mihashi, K. Kinosita, Jr and A. Ikegami, J. Mol. Biol. 179 (1984) 453.
7 K. Mihashi, A. Ooi, N. Suzuki, H. Yoshimura and K. Kinosita, Jr, Life Sci. Adv. Mol. Biol. Cell. Biol. 7 (1989) in the press.
8 K. Mihashi, J. Biochem. 96 (1984) 273.
9 N. Suzuki and K. Mihashi, Biophys. Chem. 33 (1989) 177.
10 S. Ebashi and F. Ebashi, J. Biochem. 55 (1964) 604.
11 H.E. Huxley, J. Mol. Biol. 7 (1963) 281.
12 K. Maruyama, J. Biochem. 69 (1971) 369.